CHECKING COPY

The relationship between volatile content and the eruptive style of basaltic magma: the Etna case

Paola Del Carlo and Massimo Pompilio
Istituto Nazionale di Geofisica e Vulcanologia, Sezione di Catania, Italy

Abstract
Fourier Transform Infrared (FT-IR) spectroscopic analyses of melt inclusions from four explosive eruptions of Etna (Italy) were conducted to determine pre-eruptive dissolved volatile concentrations. The studied eruptions include the 3930 BP subplinian, the 122 B.C. plinian, and the 4 January 1990 and the 23 December 1995 fountain fire eruptions. Preliminary results indicate that H_2O varies between 3.13 and 1.02 wt% and CO_2 between 1404 and 200 ppm. The most basic products (3930 BP tephra) contain the highest concentrations of CO_2 (1404 ppm), whereas fire fountain hawaiitic tephra present the lowest values (< 200 ppm) indicating a continuous degassing process during the differentiation and rising of the magma. Generally, similar behavior has been found for water, characterized by a decreasing content during the differentiation that is mainly found in the 3930 BP eruption, 1990 and 1995 fire fountain products. Considering the relevance of volatile content and behaviour in determining the eruptive style, we made some inferences on the eruptive mechanisms based on the initial high volatile content and the degassing dynamics inside the plumbing system. These two factors suggest the cause of the high explosive activity in this basaltic volcano.

Key words *melt inclusion – volatile – basaltic explosive eruptions – Etna*
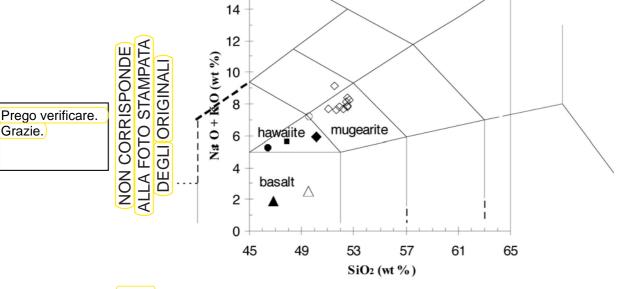
1. Introduction

Etna, located on the eastern coast of Sicily, Italy, is an active basaltic volcano characterized by quasi-persistent effusive and explosive activity. Explosive activity has usually been considered very subordinate with respect to the lava flow eruptions, but the last decade activity and some recent studies of Holocene pyroclastic deposits (Coltelli *et al.*, 1998a, 2000) indicate that explosive eruptions are quite frequent and can be very powerful. Since 1990, Etna has exhibited an extraordinarily high number of violent explosive events, including more than 150 fire fountain episodes characterized by the formation of eruptive columns from 2 to 12 km high, tephra volumes from 10^4 to 10^7 m^3 and a magnitude which ranges from intense strombolian to subplinian (Calvari *et al.*, 1991; Coltelli *et al.*, 1998b). Holocene pyroclastic succession includes many subplinian eruptions and one plinian basaltic eruption (Coltelli *et al.*, 1998a, 2000, 2003). The tephra composition is generally basaltic, ranging from picritic basalt to basic mugearite, similar to the lava flows which erupted during the same period.

It is well known that magmatic volatiles play a key role in explosive volcanism. They control vesicularity and fragmentation processes of the magma and consequently the style of the eruptions. For this reason we started to in-

Mailing address: Dr. Paola Del Carlo, Istituto Nazionale di Geofisica e Vulcanologia, Sezione di Catania, Piazza Roma 2, 95123 Catania; e-mail: delcarlo@ct.ingv.it

NON CORRISPONDE ALLA FOTO STAMPATA DEGLI ORIGINALI

Prego verificare. Grazie.

Fig. 1. Bulk rock and MI compositions in Total Alkali Silica diagram (Le Maitre, 1989). Filled triangle: 3930 B.P. scoria bulk rock; filled diamonds: 122 B.C. scoria bulk rock; filled point: 4 January 1990 scoria bulk rock; filled squares: 23 December 1995 scoria bulk rock; triangle: 3930 BP MI; diamonds: 122 B.C. MI; point: 4 January 1990 MI; squares: 23 December 1995 MI.

vestigate the amount of dissolved volatiles based on Melt Inclusion (MI) studies in some Etnean tephra. Here we report preliminary results of dissolved volatile concentrations determined by the FT-IR (Fourier Transform Infrared) spectroscopic technique and classical microanalytic methods from four explosive eruptions: the 3930 BP subplinian eruption, the 122 B.C. plinian eruption, the 4 January 1990 and the 23 December 1995 fire fountain eruptions. The 3930 BP subplinian eruption and the 122 B.C. plinian eruption represent two limiting cases in the Holocene history of Etna because the former produced the most basic magma ever erupted at Etna (picritic) whereas the latter is one of the few documented basaltic plinian eruptions in the literature. The two fire fountain episodes were typical of others which occurred in the last 13 years, and were very energetic forming eruptive columns several kilometers high. The actual activity of Etna repre-

sents a favorable case to study since we can integrate direct observations of explosive eruptions, immediate investigation and sampling of the deposits, with quantitative geophysical data (*e.g.*, seismic tremor and ground deformation) recorded by networks monitoring the volcano. Volatiles in Etna magmas have been previously investigated by various authors (Kamenetskiy *et al.*, 1986; Metrich and Clocchiatti, 1989; Metrich *et al.*, 1993; Allard *et al.*, 1994). Most of these studies focused on chlorine, sulfur and fluorine and use, with the exception of Metrich *et al.* (1993), the «difference method» (100-EMP analysis total) as an indirect estimation of H_2O and CO_2 content. However, these volatile species, being the most abundant in magma (Johnson *et al.*, 1994), have a major control over crystallization and vesiculation, density, rheology and thus eruption style (Metrich and Rutherford, 1998; Ochs and Lange; 1999; Giordano and Dingwell, 2003).

2. Volcanological and compositional features of the studied eruptions

2.1. *The 122 B.C. plinian eruption*

Tephra produced by the 122 B.C. eruption covered the entire southeastern flank of Etna, destroying the ancient town of Catania. The sequence comprises pyroclastic fall and flow deposits divided into 7 units, whose depositional characteristics, dispersal and physical parameters are reported in Coltelli *et al.* (1998a). The thickest fallout units, that represent a guide-horizon for the late Holocene stratigraphy, are C and E (from 2 to 0.3 m) formed by scoria lapilli and lithic clasts (about 20 wt%). Juvenile clasts are dense hawaiitic scoria (fig. 1), characterized by abundant, large tabular phenocrysts of plagioclase, minor olivine and rare clinopyroxene (table I); the same minerals form the groundmass with scarce, interstitial brown glass. Very rare amphibole (kaersutite) microlites are present in the whole sequence.

2.2. *The 3930 BP subplinian eruption*

The 3930 BP. subplinian eruption produced a scoria fallout with the dispersal axis toward the East (Coltelli *et al.*, 2000). The thickest deposit found (110 cm) crops out 14 km from the summit. The deposit shows a peculiar stratification due to the alternation of fine and coarse lapilli beds also marked by the change in the superficial color (brown, gray, red and purple). The deposit presents features of a distal strombolian fall layer but the thickness and dispersal indicate a greater energy of the eruption. The deposit is composed of highly vesicular, olivine-rich scoria lapilli and very rare lava lithics. The phenocryst assemblage consists of scarce (< 8%) olivine (Fo90) and minor (< 3%) Cr-diopsidic clinopyroxene. Olivine, clinopyroxene and skeletal plagioclase form microlites in hyalopilitic-cryptocrystalline groundmass (table I). The bulk rock is a picritic-basalt according to the TAS classification (La Maitre, 1989; fig. 1). The groundmass is slightly more evolved, but its composition falls on the primitive side of the basalt field. They are the most basic products ever found among Etnàs alkaline suite (Pompilio *et al.*, 1995).

2.3. *The 4 January 1990 and 23 December 1995 fire fountain eruptions*

The 4 January 1990 fire fountain eruption from South East Crater was a very powerful paroxysmal episode. It produced a copious scoria fall on the northwestern flank of the volcano reaching a deposit thickness of 60 cm about 5 km from the vent along the dispersal axis (Calvari *et al.*, 1991). Scoria are porphyritic hawaiites (fig. 1) with phenocrysts of plagioclase, clinopyroxene, olivine and microphenocrysts of Ti-magnetite (table I).

The 23 December 1995 fire fountain eruption from North East Crater produced a 9.5 km long eruptive column (Coltelli *et al.*, 1998b). The good weather conditions allowed for clear observation of the eruptive column expansion.

Table I. Mineral chemistry of the studied tephra. Microl.: microlites.

	3930 BP rim/microl.	3930 BP core	122 B.C. rim/microl.	122 B.C. core	4 January 1990 rim/microl.	4 January 1990 core	23 Dec. 1995 rim/microl.	23 Dec. 1995 core
Plg	An63-73	–	An24-85	An60-80	An86-49	An71-81	An55-86	An64-87
Ol	Fo84-88	Fo88-91	Fo70	Fo73-76	Fo70-71	Fo77-81	Fo68	–
Cpx X(di)	0.76-0.79	0.82-0.78	0.22	0.38-0.43	0.41-0.57	–	0.47-0.57	0.53-0.54
Usp%	–	–	30-48	–	–	–	–	–

The column was bent approximately 40° downwind toward the NNE and abundant lapilli and ash covered a wide area of the NE flank down to the coast producing damage to fruit plantations, cars and buildings. The deposit thickness along the main dispersal axis was 6-7 cm at 6 km from the vent and 1-2 cm at 20 km close to the Ionian coast. Lapilli and bombs were highly vesicular and glassy. Their composition is hawaiitic (fig. 1) and the mineral assemblage consists of phenocrysts of plagioclase, clinopyroxene, olivine and microphenocrysts of Ti-magnetite (table I) in a groundmass which varies from hyalopilitic to intersertal.

3. Melt inclusion analyses

3.1. *Experimental procedures*

We used Fourier Transform infrared spectroscopy (FT-IR) to determine H_2O and CO_2 concentrations in the MI's hosted in olivine phenocrysts of tephra except for the 4 January 1990 fire fountain, which was measured in a clinopyroxene phenocryst. 122 B.C. eruption carbon dioxide and water were analyzed at DST-University of Pisa in double-sided, polished MI by transmission IR spectroscopy using a Nicolet Magna-IR 560, equipped with an EverGlo source, a laser Ge-KBr beam splitter and a DTGS detector, coupled with an IR NicPlan microscope. The number of scans varied between 512 and 2048, and spectral data were collected utilizing OMNIC software. Carbon dioxide and water in 3930 BP, 4 January 1990 and 23 December 1995 eruptions were analyzed at GPS-California Institute of Technology laboratory using double-sided polished MI's and a Nicolet 60SX IR spectrometer equipped with an MCT detector, a Globar source, a KBr beam splitter, coupled to a NicPlan microscope. The number of scans varied between 1024 and 4096. Three spectra were collected on each MI, and the arithmetic mean of the resulting species concentration was calculated. Absorbance was measured from peak heights, and after subtraction of the background signal were extrapolated with a flexible drawing curve. Concentrations (C) were calculated according the Beer-Lambert law: $C = 100\ AM/(\varepsilon\rho e)$, where A is the molar absorbance, M the molar mass (g/mol), ε the molar absorptivity (L/mol cm), ρ the glass density, and e the thickness in cm. Sample thickness was measured using a digital micrometer with a precision of $\pm 1\mu m$ and checked with calibrated video analyses system. Thicknesses of each measured MI are listed in table II and vary between 10 and 82 μm. Glass density values of MI's of 2800 g/L was used for hawaiitic compositions and 2950 g/L for the basaltic one.

Water is dissolved as molecular water ($H_2O_{mol.}$) and hydroxyl group (OH^-) in the MI. The concentrations of total water ($H_2O_{mol.} + OH^-$) in MI were determined using the broad band at 3535 cm^{-1} of the total water. The values for molar absorptivity ε^{3535} used is 63 ± 3 L/mol cm determined for basaltic alkaline glass according to Dixon *et al.* (1995). Carbon dissolved in MI is present only as CO_3^{-2} which gives the doublet absorption band at 1350-1430 and 1450-1570 cm^{-1}. The value for molar absorptivity ε^{1350} used is 375 ± 20 L/mol cm according to Fine and Stolper (1986).

Minerals and glass composition were analyzed using an Energy Dispersive Analytical (LINK eXl) spectrometer linked to the Cambridge Stereoscan 360 SEM, and quantitative analyses were obtained by ZAF correction using natural standard for the calibration. Analytical conditions were 15 keV of acceleration tension, 500 pA of probe current. Glass was analyzed using a raster of about 10×10 micron area in order to minimize Na loss. Replicate analyses of internal natural standards (mineral and glasses) assured an analytical precision of less than 1% for SiO_2 and Al_2O_3, about 2% for FeO, MgO and CaO, and from 3-5% for remaining elements. Due to the lower value ($< 0.5\%$), chlorine and sulfur concentration obtained from SEM analyses must be considered only semi-quantitative and was not used for the discussion. Table II lists the major element compositions and dissolved volatile concentrations of the studied MI.

4

Table II. Melt inclusion compositions. H_2O and CO_2 from FT-IR analyses. Bdl: below detection limit. S detection limit is ±100 ppm, *=Mg# in host clinopyroxene crystal.

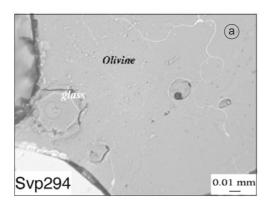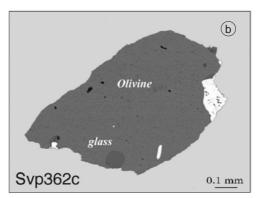| Eruption	3930 BP											122 B.C.	4 Jan. 1990	23 December 1995	
Inclusion	294	362a	362b	362ca	362cb	362cc	363da	363a	363b	363c	363d	367a	se66	231295b	231295
Thickness (micron)	17	37	20	10	10	10	20	13	31	33	20	31	22	65	82
SiO_2	45.62	49.91	51.26	50.25	50.20	50.07	49.87	49.97	50.50	52.54	49.90	51.15	46.56	47.27	51.41
TiO_2	1.00	1.76	1.78	1.66	1.64	1.69	1.70	1.75	1.70	1.81	1.72	1.72	2.14	1.31	1.52
Al_2O_3	10.18	15.94	16.52	16.65	16.29	16.08	17.47	16.11	16.94	16.37	16.14	16.57	15.64	18.43	15.39
FeOtot	7.36	8.89	8.04	7.54	7.84	7.77	8.75	8.06	7.39	7.50	8.44	7.58	9.69	9.25	9.93
MgO	11.20	3.98	3.64	3.71	3.85	3.84	4.08	4.11	3.72	3.52	4.01	3.68	3.69	3.74	2.94
CaO	13.28	7.05	6.94	7.77	7.10	7.18	6.97	6.89	6.44	6.41	6.86	6.97	8.46	8.90	6.35
Na_2O	1.60	4.94	5.40	5.34	5.48	5.37	5.30	6.48	5.86	3.88	5.25	5.62	4.08	4.58	5.34
K_2O	0.74	2.39	2.53	2.07	2.04	2.08	2.23	2.39	2.18	2.22	2.27	2.38	2.65	3.01	2.71
P_2O_5	0.49	1.09	1.18	0.75	0.68	0.79	0.80	0.84	0.95	1.19	0.94	0.94	0.82	0.86	1.04
S	0.40	0.18	0.16	0.20	0.16	0.18	0.19	0.15	0.20	bdl	0.20	0.18	bdl	0.24	bdl
Cl	0.29	0.35	0.27	0.35	0.34	0.32	0.32	0.28	0.29	0.29	0.30	0.33	0.15	0.35	0.25
H_2O	2.45	2.22	1.02	2.25	2.86	3.13	1.26	1.56	2.63	3.04	2.55	1.94	1.93	1.85	1.63
CO_2 ppm	1404	272	283	503	880	576	289	451	266	207	615	221	3	210	bdl
Fo (%)	90	73	73	75	74	75	74	75	75	74	74	74	0.73*	75	68

3.2. *MI features*

Abundant MI of variable size were found in olivine crystals from 122 B.C. tephra. Those chosen for this study are about 100 μm in maximum diameter. Many others were observed but were too small to be prepared and measured by FT-IR spectroscopy. They are generally glassy, although some show limited crystallization of olivine and clinopyroxene around the border. Inclusions in olivine crystals of 3930 BP tephra are generally rare and very small. Quite often they appear empty as original trapped fluid or vapor and leaked. In a few favorable cases, where glass was trapped, the inclusions show negative crystal shapes and contain shrinkage bubbles. In 23 December 1995 olivine crystal MI's are more abundant and show quite often negative crystal or a sub-rounded shapes ac-companied by shrinkage bubbles of variable sizes. No mineral inclusions are present in these MI. In the sample from the 4 January 1990 tephra, some large «hourglass» inclusions (Anderson, 1991) with small trapped crystals, were found in diopside crystals.
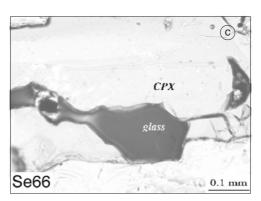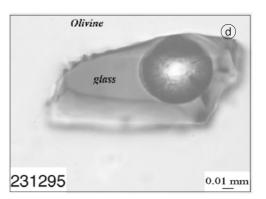
3.3. *MI composition*

A MI analyzed from the 3930 BP subplinian eruption was trapped in high forsteritic olivine (Fo90) and has basaltic composition (fig. 1). This inclusion contains 2.45 wt% H_2O and 1404 ppm CO_2. Partitioning of Fe and Mg between olivine and MI (K_d 0.33) is close to equilibrium value for crystallization at depth (Mysen, 1975).

The most complete set of measurements was carried out on products of the 122 B.C.

Fig. 2a-d. Photo of a) MI in 3930 BP tephra; b) photo of MI in 122 B.C. tephra; c) photo of MI in 4 January 1990 tephra; d) photo of MI in 23 December 1995 tephra.

plinian eruption (Del Carlo, 2001). MI have mugearite composition (fig. 1). The measured H_2O concentrations range between 1.02 and 3.13 wt% and CO_2 between 207 and 880 ppm. The host olivine has a homogeneous composition (Fo72-75). Partitioning of Fe and Mg (K_d 0.17-0.25) between olivine and trapped glass indicates that the inclusions suffered only limited post-entrapment crystallization (< 6%).
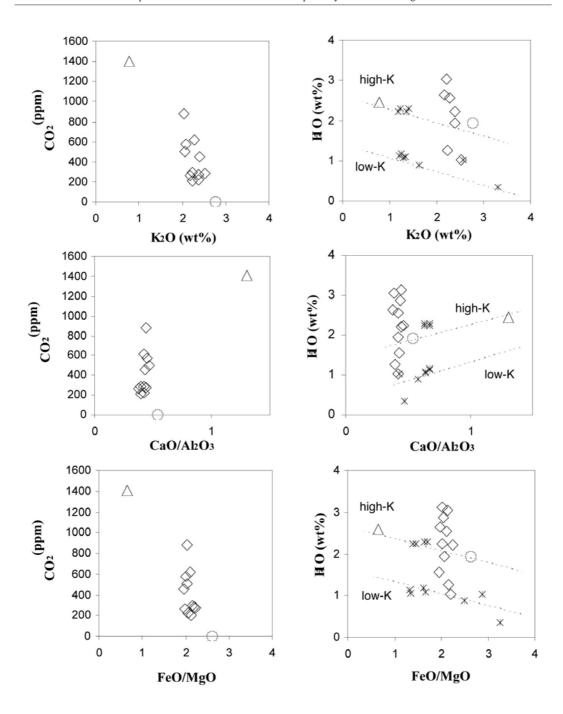
MI studied in 1990 fire fountain tephra is hosted in diopside crystal. The melt has a hawaiitic/basic mugearitic composition (fig. 1) and contains 1.93% H_2O and CO_2 below detection.

MI's measured in 1995 fire fountain tephra was trapped in olivine crystals with Fo68-75. One MI has a mugearitic composition (fig. 1) and contains 1.63% H_2O. The other has a lower alka-

li and silica content but a higher water concentration of 1.85 wt%. An appreciable CO_2 content (210 ppm) was measured only in MI within olivine with Fo75. Partitioning of Fe and Mg between olivine and MI (K_d 0.27-0.28) indicates, as in 122 B.C. MI, equilibrium between host minerals and trapped liquid and excludes significant post-entrapment crystallization of host olivine.

On the whole, for the studied MI the occurrence of extensive post-entrapment crystallization can be ruled out, therefore the measured volatile concentrations represent the volatile content of the magma at the time of entrapment.
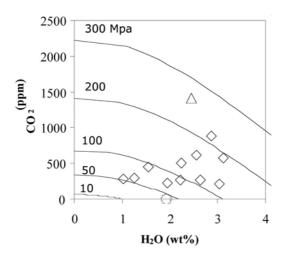
Figure 3 shows the relationships between volatiles and single element or element ratios, that change during the differentiation process. Taking into account the whole set of measure-

Fig. 3. Correlations between CO_2 and H_2O *versus* K_2O composition, CaO/Al_2O_3 ratio and FeO/MgO ratio in MI from the studied tephra. Symbols as in fig. 1. Stars: data from Metrich *et al.* (1993).

ments that span in composition from basalt to hawaiite, or the more restricted compositional range observed in the 122 B.C. MI's, a general inverse correlation exists between CO_2 and K_2O and FeO-MgO ratio (fig. 3). K_2O is considered to be incompatible in the magma, and is expected to increase during the differentiation. Likewise the FeO/MgO ratio is expected to increase in the melt due to crystallization of mafic phases, while pyroxene and plagioclase precipitation would diminish the CaO/Al_2O_3 ratio in the melt. In the CO_2 *versus* K_2O and FeO/MgO diagrams (fig. 3), the scatter is limited and all the inclusions plot along a single correlation curve. This pattern is compatible with the concomitant occurrence of differentiation and CO_2 loss from the magma, occurring during the ascent and cooling of a magma saturated in CO_2. A similar general relationship is observed using H_2O as volatile species in these diagrams. On the whole, the sign of the correlation does not change, but the scatter is large and not a single correlation curve can be drawn.

In particular, in 122 B.C. MI's, we observe a fast decrease in water content coupled with a small changes in compositional parameter related to differentiation, indicating that they are poorly dependent of composition. This is compatible with a rapid decompression and water exsolution accompanied by limited cooling and crystallization processes for the magma feeding the 122 B.C. eruption. A different trend, characterized by a decrease of water during the differentiation, is depicted by 3930 BP, 1990 and 1995 MI's. The high-K MI's compositions of Metrich *et al.* (1993), that correspond to recent Etna products, fall in the same trend. Instead, the low-K MI's of Metrich *et al.* (1993) define another trend with a comparable slope but shifted toward lower water content (fig. 3).

Noteworthy is that the inclusion with the most primitive composition does not have the higher water content. This implies that the first (probably deep) differentiation stage that produced the less evolved melts between the 122 B.C. MI, from a primitive magma, such as that feeding the 3930 BP eruption, must have developed in conditions of water undersaturation.

Assuming that the measured volatile content represents the maximum amount dissolved in magma, a minimum pressure of entrapment can be calculated following Dixon and Stolper (1995) and a H_2O and CO_2 solubility model (fig. 4). In fig. 4, the highest pressure (≈ 260 Mpa) is associated with the inclusion in the 3930 BP tephra, which is the most basic magma, while the lowest one (< 50 Mpa) corresponds to the 23 December 1995 fire fountain products. Inclusions in crystals of 122 B.C. eruption show a large variation in volatile content that corresponds to a trapping pressure ranging from 210 to 50 Mpa.

4. Discussion

Volatile contents (H_2O and CO_2) found in Etna tephra are on average higher than those found in other intra-plate basaltic magmas known in literature, such as Kilauea (Hawaii) with 0.1-1 wt% of H_2O and comparable CO_2 content. Previous work on dissolved volatiles from Etnean magmas reported similar water concentrations. For example, Metrich *et al.* (1993) found for the 1989-90 fire fountain tephra 1.1 wt% of water and in the 1892 eruption 2.3 wt% of water. Thus,

Fig. 4. H_2O (wt%) *versus* CO_2 (ppm) diagram. Saturation curves at different pressures are represented according to Dixon and Stolper (1995) model for alkaline magmas. Symbols as in fig. 1.

the initial high volatile content and the degassing dynamics inside the plumbing system may have a major role in controlling the eruptive style of Etna suggesting the cause for the high explosive activity in this basaltic volcano.

Inferences on the eruptive mechanisms can be proposed on the basis of the inverse correlation between volatiles and incompatible elements (*e.g.*, K_2O) or indexes of differentiation (*e.g.*, FeO/MgO). These relationships suggest: i) the devolatilisation processes take place while the differentiation is going on; ii) magmas feeding the explosive eruptions are saturated in both (H_2O and CO_2) investigated volatile species. This pattern even with a distinct rate is visible also in the two evolution trends (high-K and low-K) found by Metrich *et al.* (1993) in MI's analysed in recent Etnean volcanics.

The trend in the H_2O-CO_2 diagram (fig. 4) suggests a devolatilisation in a closed system more than an open system. In addition, a large pressure range would exclude the entrapment of MI forming in shallow magma chamber (fig. 4), and further indicate that devolatilisation and degassing occurred in non-equilibrium conditions. These effects are more visible in the 122 B.C. eruption, where a large variation of volatile content is not accompanied by significant changes in MI composition, suggesting limited cooling, crystallization and differentiation processes associated with a fast uprising.

Normally, the rheological properties and the volatile content of basaltic magmas do not allow plinian eruptions, but the sudden decompression of a basaltic magma may cause the nucleation of a large number of bubbles that rapidly increase bulk viscosity and reduce magma density allowing rapid ascent in the conduit. Disruption of low density vesicular magma results in a pyroclastic mixture leading to the formation of a plinian eruptive column. This is the case of the 122 B.C. eruption, for which a sudden decompression model of the large magma body was proposed in Coltelli *et al.* (1998a) to form a plinian eruption. The whole 122 B.C. magma was volatile saturated with an incipient vesicularity. In this condition, even a small decompression of the system could have caused the gas to be exsolved, although the pre-eruptive water content was quite low (about 1 wt%). At low magma ascent rates,

gas separates from low-viscosity melt and bubbles coalesce during the ascent producing the explosion of large bubbles forming strombolian activity. Conversely, rapid ascent rates in basaltic magmas prevent bubble coalescence and can produce fire fountains and, if the volume is greater, subplinian and plinian eruptions. So, different paths of decompression of initially similar magmas may deeply influence the eruptive style.

5. Conclusions

The explosive activity of Etna represents a continuous hazard for lands and villages located on its flanks. The most recent eruption, which started on 27 October 2002, gives an excellent example having produced a continuous ash emission for more than two months and causing damage to the eastern Sicily economy mainly related to the prolonged closure of Catania airport. So, understanding of the triggering mechanisms of high explosive basaltic eruptions is of fundamental importance in order to assess the probability of future, large explosive events.

This study on MI in minerals provided useful information on differentiation and degassing processes that occur during the storage and ascent of magma before the eruption, in particular the relationships between volatile content and composition. This preliminary study outlines that initial volatile content at Etna is higher than in other basaltic volcanoes indicating their important role in controlling the eruptive style. We made also some inferences on the eruptive mechanisms based on the initial high volatile content and the degassing dynamics inside the shallow plumbing system, indicating these two factors as the cause of the high explosive activity in this basaltic volcano.

REFERENCES

ALLARD, P., J. CARBONNELLE, N. METRICH, H. LOYER and P. ZETTWOOG (1994): Sulfur output and magma degassing budget of Stromboli Volcano, *Nature*, **368** (6469), 326-330.

ANDERSON, A.T. (1991): Hourglass inclusion: Theory and application to the Bishop rhyolitic Tuff, *Am. Mineral.*, **76**, 530-547.

CALVARI, S., M. COLTELLI, M. POMPILIO and V. SCRIBANO (1991): Etna: the eruptive activity between October 1989 and December 1990, *Acta Vulcanol.*, **1**, 257-260.

COLTELLI, M., P. DEL CARLO and L. VEZZOLI (1998a): Discovery of a Plinian basaltic eruption of Roman age at Etna volcano, Italy, *Geology*, **26**, 1095-1098.

COLTELLI, M., M. POMPILIO, P. DEL CARLO, S. CALVARI, S. PANNUCCI and V. SCRIBANO (1998b): Mt. Etna – 1993-1995 eruptive activity, *Acta Vulcanol.*, **10** (1), 141-148.

COLTELLI, M., P. DEL CARLO and L. VEZZOLI (2000): Stratigraphic constraints for explosive activity in the past 100ka at Etna Volcano, Italy, *Int. J. Earth Sci.*, **89**, 665-677.

COLTELLI, M., P. DEL CARLO and L. VEZZOLI (2003): Tephrostratigraphy and chronology of Etna (Italy) in the last 12 ka: implications for volcanic history and hazard (in press).

DEL CARLO, P. (2001): The 122 B.C. Etna Plinian eruption: magmatic processes and eruptive dynamics on the base of chemical, petrographical and volcanological data. *Plinius*, **25**, 39-43.

DIXON, J.E. and E.M. STOLPER (1995): An experimental study of water and carbon dioxide solubilities in mid-ocean ridge basaltic liquids. Part II: Applications to degassing, *J. Petrol.*, **36**, 1633-1646.

DIXON, J.E., E.M. STOLPER and J.R. HOLLOWAY (1995): An experimental study of water and carbon dioxide solubilities in mid-ocean ridge basaltic liquids. Part I: Calibrations and solubility models, *J. Petrol.*, **36**, 1607-1631.

FINE, G. and E. STOLPER (1986): Dissolved carbon dioxide in basaltic glasses: concentration and speciation, *Earth Plan. Sci. Lett.*, **76**, 263-278.

GIORDANO, D. and D.B. DINGWELL (2003): Viscosity of hydrous Etna basalt: implications for Plinian-style basaltic eruptions, *Bull. Volcanol*, **65** (1), 8-14.

JOHNSON, M.C., A.T. ANDERSON and M.J. RUTHERFORD (1994): Pre-eruptive volatiles contents of magmas, in *Volatiles in Magmas,* edited by M.R. CARROLL and J.R. HOLLOWAY, *Rev. Mineral.,* Min. Soc. America, Washington, **30**, 281-330.

KAMENETSKIY, V., A. SOBOLEV, R. CLOCCHIATTI and N. METRICH (1986): Prémiere estimation de la teneur en eau du magma de l'Etna à partir de l'étude des inclusions vitreuses et fluides, *Compte Rendue de l'Academie de Sciences Paris*, **302** (2), 1069-1074.

LE MAITRE, R.W. (1989): A classification of igneous rocks and glossary of terms, *Blackwell Scient. Publ.*, Oxford, pp. 193.

METRICH, N. and R. CLOCCHIATTI (1989): Melt inclusion investigation of the volatile behaviour in historic alkali basaltic magmas of Etna, *Bull. Volcanol.*, **51**, 185-198.

METRICH, N. and M.J. RUTHERFORD (1998): Low pressure crystallization paths of H_2O-saturated basaltic-hawaiitic melts from Mt Etna: Implications for open-system degassing of basaltic volcanoes, *Geochim. Cosmochim. Acta*, **62** (7), 1195-1205.

METRICH, N., R. CLOCCHIATTI, M. MOSBAH and M. CHAUSSIDON (1993): The 1989-1990 activity of etna magma mingling and ascent of H_2O-CL-S-rich basaltic magma - evidence from melt inclusions, *J. Volcanol. Geotherm. Res.*, **59** (1/2), 131-144.

MYSEN, B.O. (1975): Partitioning of iron and magnesium between crystals and partial melts in peridotite upper mantle, *Contrib. Mineral. Petrol.*, **52** (2), 69-76.

OCHS, F.A. and R.A. LANGE (1999): The density of hydrous magmatic liquids, *Science*, **283**, 1314-1317.

POMPILIO, M., M. COLTELLI, P. DEL CARLO and L. VEZZOLI (1995): How do basaltic magmas feeding explosive eruptions rise and differentiate at Mt. Etna?, *Per. Mineral.*, **64**, 253-254.

Se possibile completare. Grazie.